Performance Analysis of the Flying Wing Airfoils

PRISACARIU Vasile
Henri Coandă Air Force Academy, Brașov, Romania, aerosavelli73@yahoo.com

Abstract
Flying wings flight performances depend directly on the 2D aerodynamic optimization (choosing aerodynamic profile). The aerodynamic profiles used in tailless aircraft have a series of specific constructive performance. This article presents a piece of analysis regarding the 2D aerodynamic profile used in the construction of a flying wing UAV type.

Keywords
aerodynamic analysis, Phoenix airfoil, XFLR5, Profili 2.21

Notations of symbols

MAC	- main aerodynamic chord	AoA	- angle of attack
C_l	- lift coefficient	ρ	- air density
C_m	- moment coefficient	R_e	- Reynolds number
C_d	- drag coefficient	υ	- kinematics viscosity
C_p	- pressure coefficient	v, V	- air speed , forwards, on airfoil

1. Introduction

Phoenix profile (Phönix) as specialty reference [1, 3, 8] is used in the construction of aircraft (propelled and non-propelled), both classic and tailless concept, especially the "plank" wings without angle arrow but with some torsion angle at the end of the plan (0° ÷ -5°), see Figures 1, 2 and Table 1.

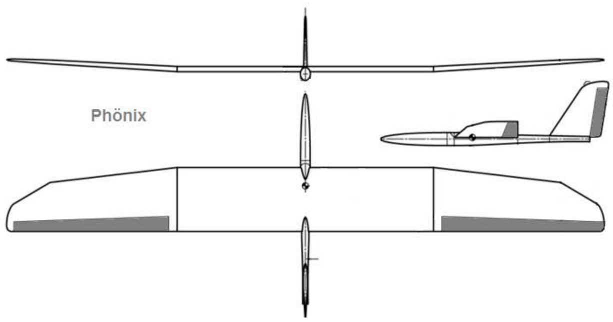

Fig. 1. Model RC Phönix

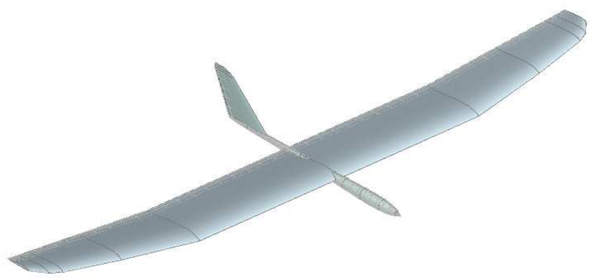

Fig. 2. XFLR5 model [5]

Table 1. Glider RC Phoenix characteristics

Span	2800 m	Aspect ratio	10.34
M.A.C.	277 mm	Max weight	2 kg

Phoenix is part of the aerodynamic profiles relatively thin (thickness below 10%), used in tailless aircraft, which also includes Eppler 221 (thickness 9.39%), MH 62 (9.30%), EH1.5 / 9.0 (thickness 9%) and PW 51, show Figure 3 [7, 8].

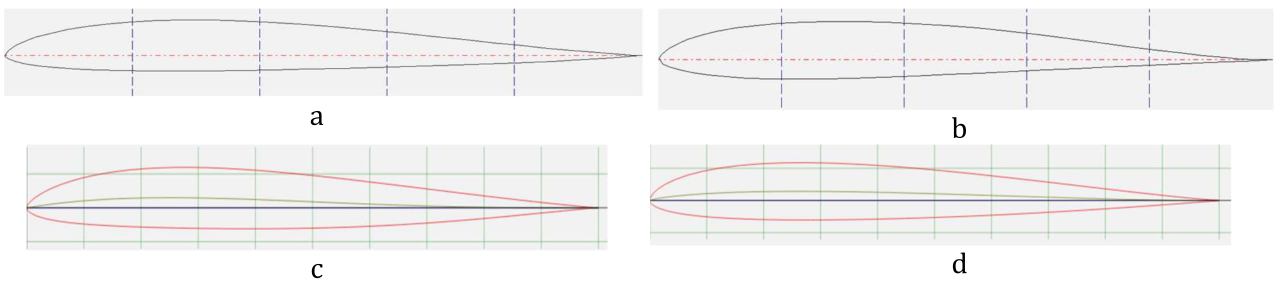

Fig. 3. Eppler 221 (a), MH 62 (b), EH 1.5/9.0 (c), PW 51 (d)

2. 2D Aerodynamic Analysis

Propose to analyze the Phoenix (Phönix) profile used in flying wings (Figure 3). The data input required for aerodynamic analysis is listed in Table 2 [3].

Table 2. Phoenix input data

Maximum thickness (chord)	8.19%	Maximum deflection	2.78
Coordinate for the maximum thickness	27.5%	Coordinate for the maximum deflection	25%

Aerodynamic analysis conditions are: Reynolds no., altitude, flight velocities and the aerodynamic average chord, listed in Table 3.

Table 3. Aerodynamic analysis conditions

MAC (mm)	600	Speed (m/s)	10÷30
Altitude (m)	100	R_e	$4\times10^5 \div 12\times10^5$
Density ρ	1.22 kg/m³	Kinematics viscosity υ	14.6×10^{-6}

2.1. 2D Javafoil analysis

Javafoil is a tool known for Xfoil code, [2, 6] code that delivers results with a high degree of confidence. Phoenix profile is highlighted in Figure 4 and the results are recorded in the graphs in Figure 5.

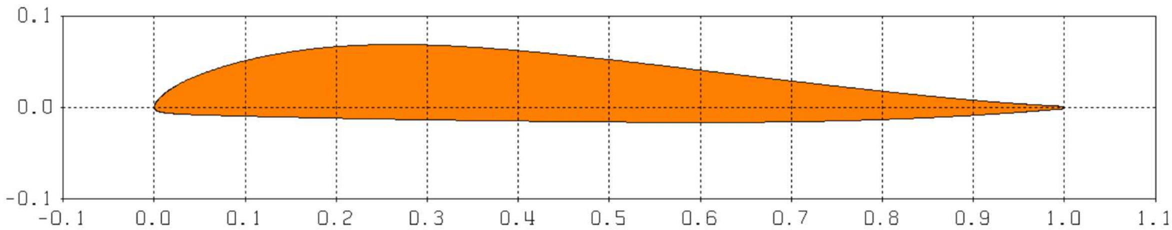

Fig. 4. Phoenix airfoil

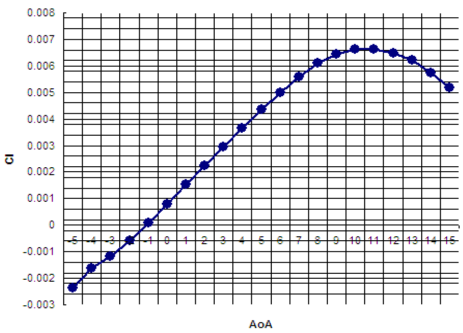

C_l-AoA

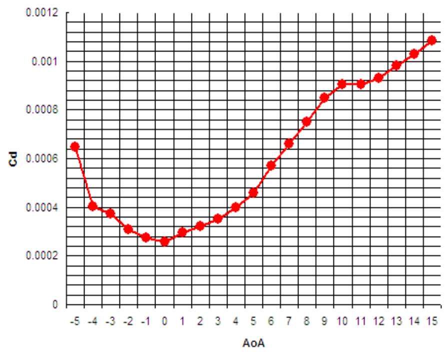

C_d-AoA

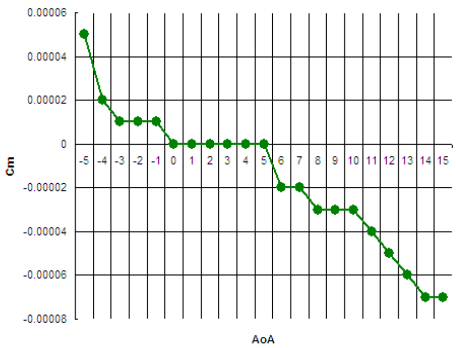

C_m-AoA

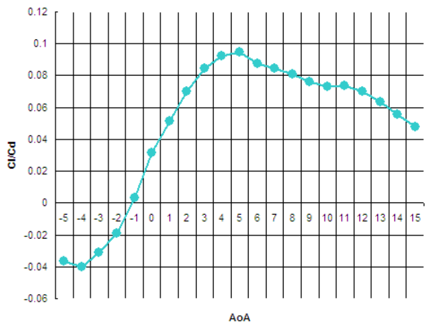

(C_l/C_d)-AoA

Fig. 5. Phoenix airfoil aerodinamics performances

In figure 6 can see the C_p distributions and speed ratio (v_∞/V), depending on the incidence angle (AoA), four cases (various AoA).

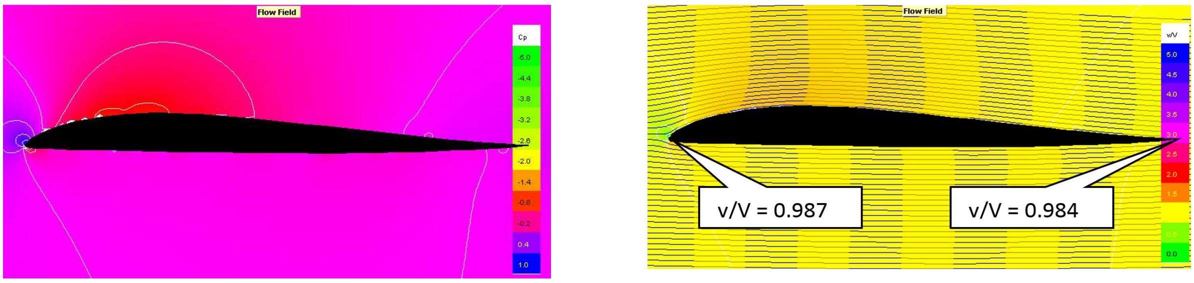

AoA = 0°

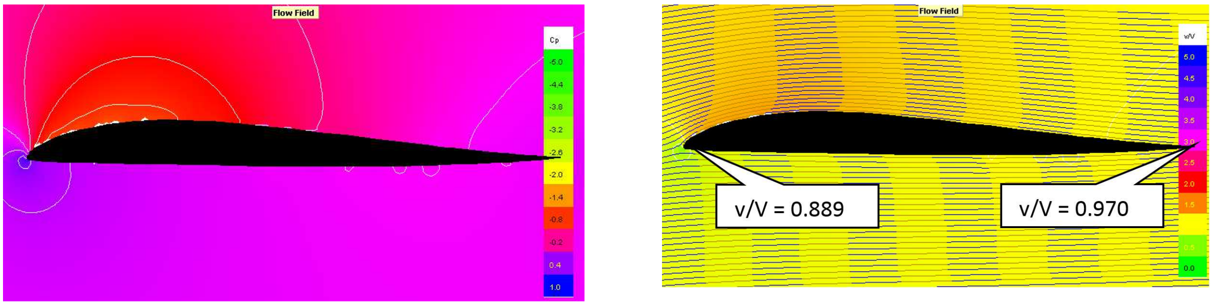

AoA = 3°

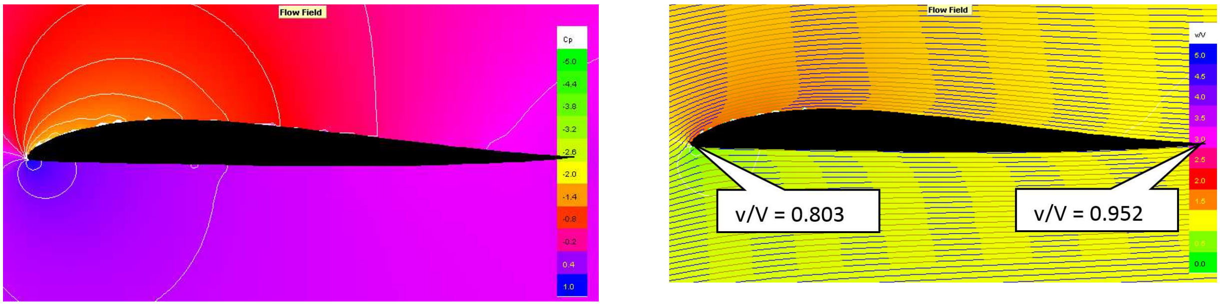

AoA = 6°

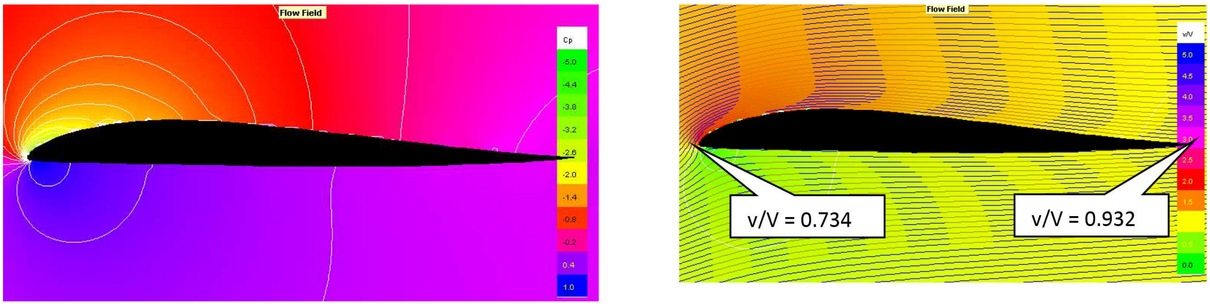

AoA = 9°

Fig. 6. C_p-AoA (left), v_∞/V-AoA (right)

Following the Figure 6 distribution of pressure coefficient (Cp-AoA), can observe the development of the low pressure gradient in the first third of the rear profile with implications for the boundary layer and significant reduction of the speed distribution (v_∞/V-AoA), leading the edge from 0.987 to 0.734.

2.2. 2D Profili 2.2 analysis

Analysis of 2D (airfoil) is achieved by means of the software tool Profili 2.21 [4, 10]. The aerodynamic profile analysis was performed at three base speeds (10 m/s, 20 m/s, 30 m/s) with tree R_e, and generated polar in Figures 7, 8 and 9.

In Figure 7 can see values of the coefficient of lift (C_l) versus coefficient of drag (C_d). C_l values has a maximum (1.2) for C_d=0.03 (AoA=3^0, Figure 8).

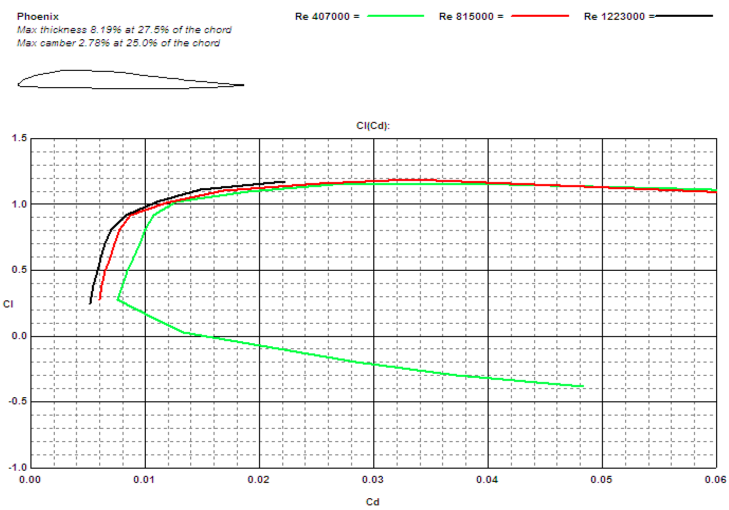

Fig. 7. C_l-C_d (for various R_e)

In Figure 8 observe an almost identical polar for the three flight speeds, the coefficient of lift has a maximum value (1.4) and at an incidence of 11°.

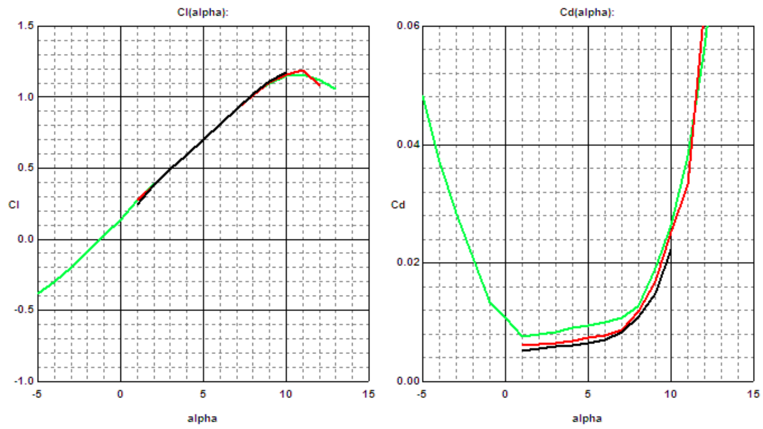

Fig. 8. C_l-AoA, C_d-AoA (for various R_e)

In Figure 9 can see a fine maximum (C_l/C_d-AoA) at an incidence of 6^0 to 30 m/s, 7°-20 m/s and 10 m/s, while the moment (C_m) has it's graphs almost 0 and positive values are observed at 11^0 (0.01). The drag coefficient (C_d) has a significant linear increase from an incidence of 8°. Incidence versus coefficient values is shown in the Table 4.

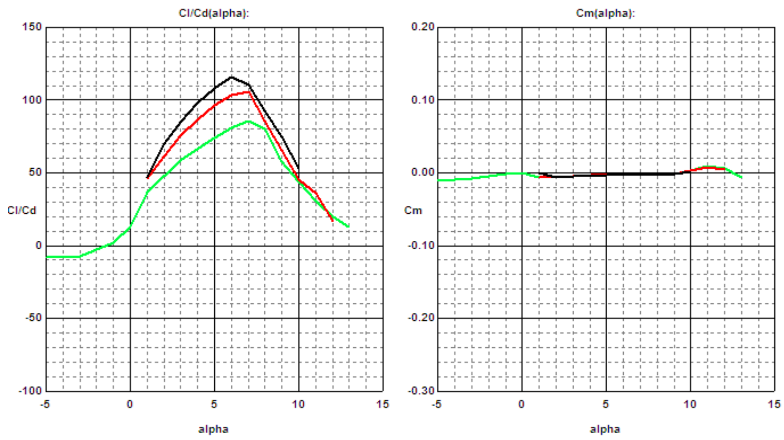

Fig. 9. C_l/C_d-AoA, C_m-AoA (for various R_e)

Table 4. Phoenix airfoil coefficients

Phoenix - Re = 407000				
Alfa	Cl	Cd	Cl/Cd	Cm
-5.0	-0.3793	0.0483	-7.8530	-0.0109
-4.0	-0.2975	0.0372	-7.9973	-0.0097
-3.0	-0.1966	0.0284	-6.9225	-0.0074
-1.0	0.0243	0.0133	1.8271	-0.0017
0.0	0.1342	0.0107	12.5421	0.0000
1.0	0.2788	0.0076	36.6842	-0.0067
3.0	0.4902	0.0084	58.3571	-0.0048
4.0	0.5958	0.0090	66.2000	-0.0039
5.0	0.7020	0.0095	73.8947	-0.0032
6.0	0.8094	0.0100	80.9400	-0.0029
7.0	0.9162	0.0107	85.6262	-0.0028
8.0	1.0164	0.0127	80.0315	-0.0028
9.0	1.0946	0.0190	57.6105	-0.0011
10.0	1.1515	0.0264	43.6174	0.0030
11.0	1.1604	0.0381	30.4567	0.0096
12.0	1.1224	0.0564	19.9007	0.0066
13.0	1.0604	0.0808	13.1238	-0.0062

Phoenix - Re = 815000				
Alfa	Cl	Cd	Cl/Cd	Cm
1.0	0.2768	0.0060	46.1333	-0.0064
2.0	0.3836	0.0062	61.8710	-0.0056
3.0	0.4897	0.0065	75.3385	-0.0047
4.0	0.5959	0.0069	86.3623	-0.0038
5.0	0.7025	0.0073	96.2329	-0.0032
6.0	0.8101	0.0078	103.8590	-0.0030
7.0	0.9173	0.0087	105.4368	-0.0031
8.0	1.0147	0.0118	85.9915	-0.0032
9.0	1.1019	0.0168	65.5893	-0.0015
10.0	1.1548	0.0253	45.6443	0.0031
11.0	1.1923	0.0333	35.8048	0.0081
12.0	1.0812	0.0635	17.0268	0.0042

Phoenix - Re = 1223000				
Alfa	Cl	Cd	Cl/Cd	Cm
1.0	0.2437	0.0052	46.8654	0.0007
2.0	0.3839	0.0055	69.8000	-0.0057
3.0	0.4902	0.0058	84.5172	-0.0048
4.0	0.5961	0.0061	97.7213	-0.0039
5.0	0.7026	0.0065	108.0923	-0.0033
6.0	0.8102	0.0070	115.7429	-0.0030
7.0	0.9160	0.0083	110.3614	-0.0032
8.0	1.0157	0.0110	92.3364	-0.0034
9.0	1.1099	0.0148	74.9932	-0.0022
10.0	1.1742	0.0222	52.8919	0.0018

Aerodynamic profile behaviour on the terms proposed in Tables 2 and 3 were analyzed even for turning flap at 5° and 10° values (joint at 20% of the chord). Polar are shown in Figures 10, 11 and 12.

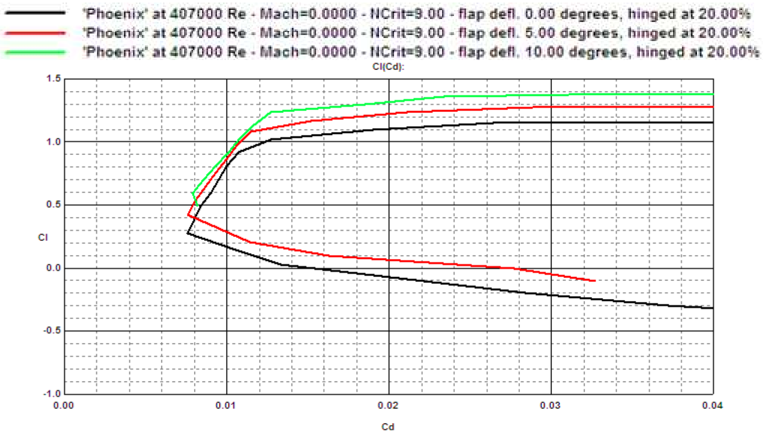

Fig. 10. C_l-C_d

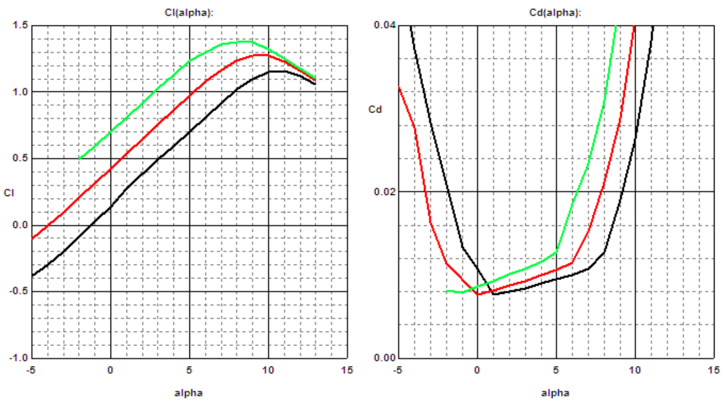

Fig. 11. C_l-AoA, C_d-AoA

Polar with turning profile influence the coefficient of lift flap, it increases from 1.25 (turning 0° and incidence 10.5°) to 1.6 (turning 5° and incidence 9.5°) and 1.8 (turning 10° and lifting 8°). Drag coefficient (Figure 11) increased from 0.015 (8° turning 0° and incidence) to 0.015 (incidence turning 5° and 6°) and 0.016 (turning 10° and lifting 5°). Aerodynamic finesse, increases with the steering angle to decrease the incidence (7°, 6°, 5°).

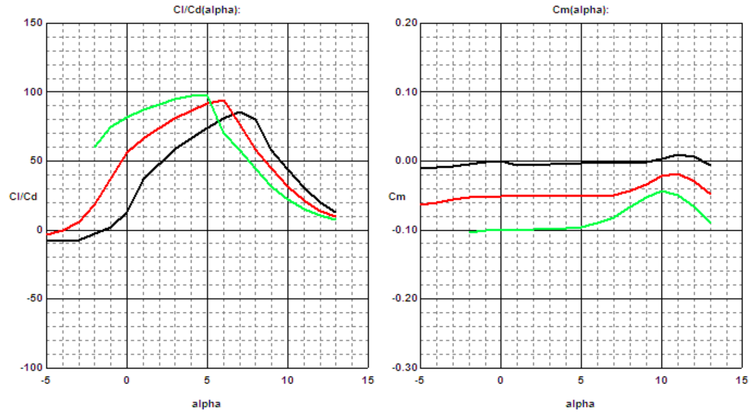

Fig. 12. C_l/C_d-AoA and C_m-AoA

The moment coefficient has values close to 0, steering flap 5° which leads to a C_m of 0.05 occurrence of –2° ÷ 7° with a significant decrease to -0.02, turning flap 10° creating a constant C_m=0.10 value (see Figure 12), for AoA= –2°÷ 4° with a decrease to 0.04 for an incidence of 10°.

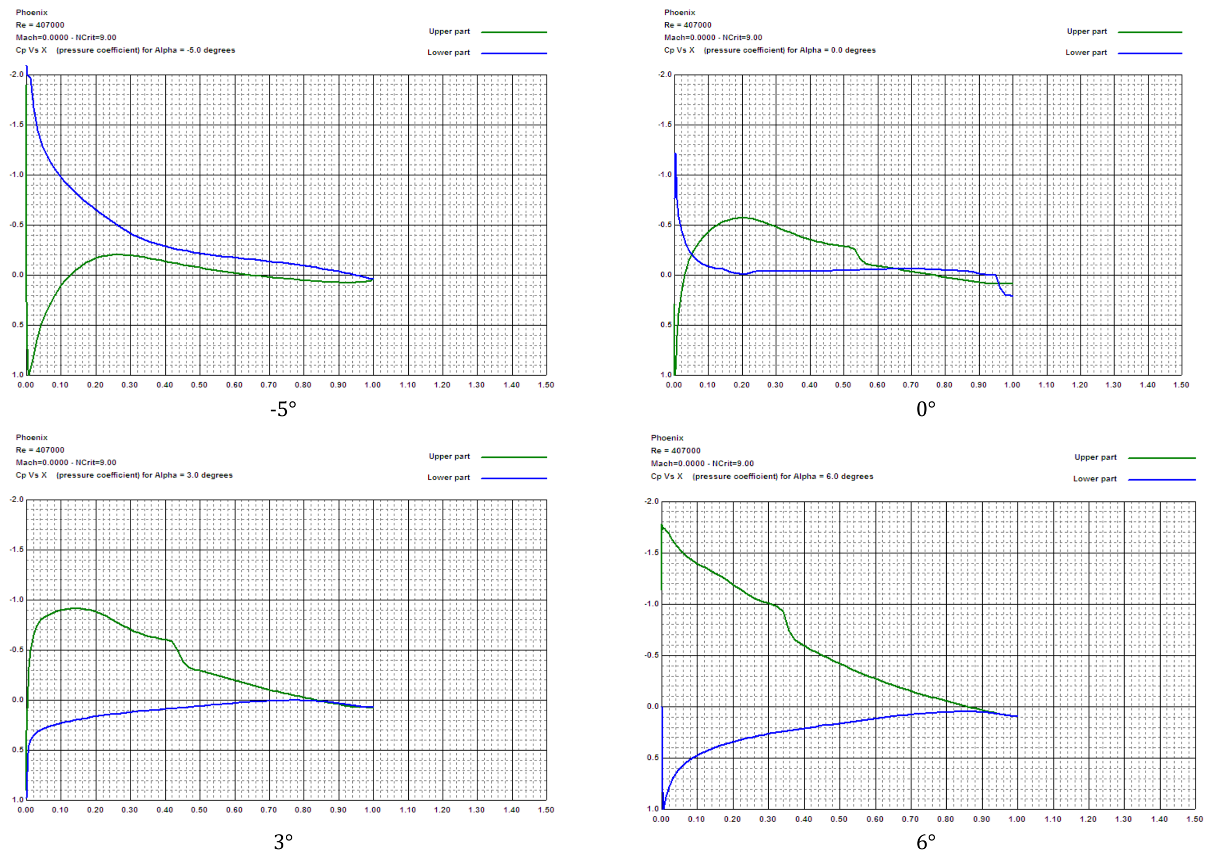

Fig. 13. Pressure coefficient (C_p) and chord airfoil versus incidence (AoA)

Figure 13 shows coefficient of pressure (C_p) versus chord for airfoil at R_e=407000 in four AoA, C_p variation can be seen for upper part and lower part, C_p values differences increase for AoA at 6^0.

2.3. 2D Analysis with XFLR5

XFLR5 is used as a tool for performance analysis freeware 2D profile and 3D geometries, generating relevant pre-analyze aerodynamic phase results [9, 11].

The following charts (figure 14, 15, 16 and 17) reveal variation of major coefficients (C_l, C_d, C_m and C_l/C_d) versus incidence (AoA) that characterize the Phoenix airfoil for AoA between -5^0 and 15^0.

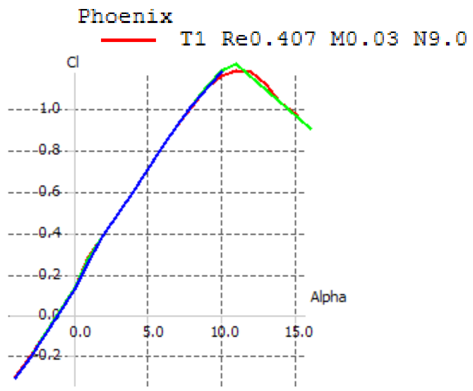

Fig. 14. C_l-AoA

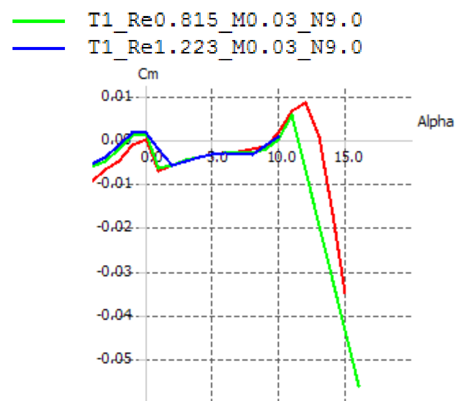

Fig. 15. C_m-AoA

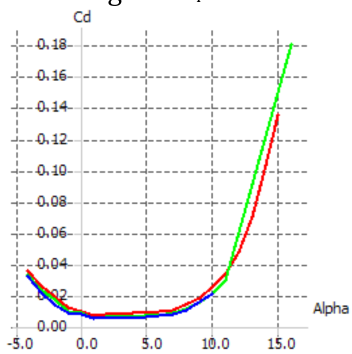

Fig. 16. C_d-AoA

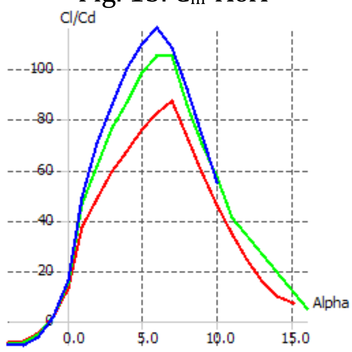

Fig. 17. C_l/C_d-AoA

Figure 14 shows the lift coefficient is maximum (1.25) at an incidence of 12° (10 m/s) and for 20 m/s and 30 m/s have a value of 1.3 lifting at 15° incidence (AoA) and longitudinal moment C_m (Figure 15) have optimum values for AoA=0÷11^0. Drag coefficient C_d increase for AoA>11^0 (Figure 16), from Figure 17 results a maximum gliding ratio to 7°, [5, 11].

4. Conclusions

For a complete evaluation we will present in following matters some comparative results regarding the three evaluation software, see Figures 18, 19, 20 and 21.

Although the three assessment tools are based on software code Xfoil graphs in Figures 18, 19, 20 and 21, they also reveal significant differences in some performance indicators. These differences are different approaches to the original simulation and the degree of refinement on the final data for each software tool [6].

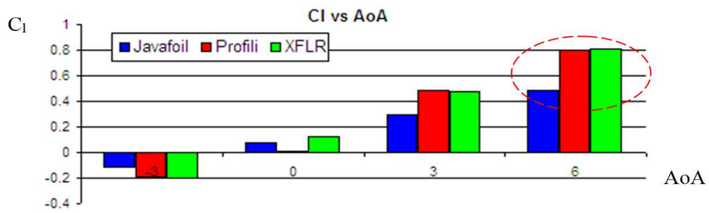

Fig. 18. Comparative data C_l-AoA

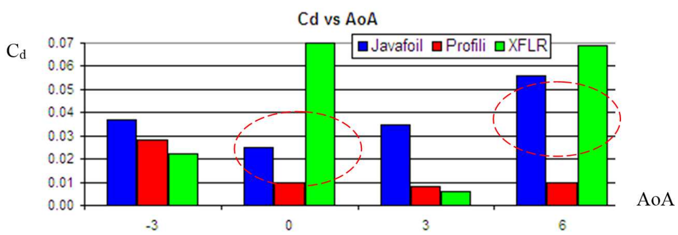

Fig. 19. Comparative data C_d-AoA

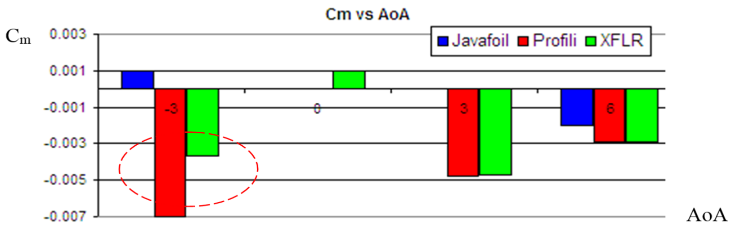

Fig. 20. Comparative data C_m-AoA

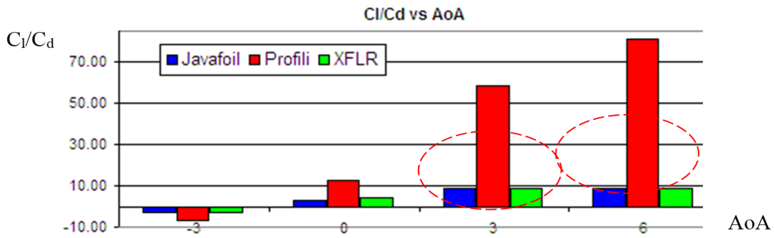

Fig. 21. Comparative data C_l/C_d-AoA

Although software tools that are based on code Xfoil that has its own database are limited to an analysis of 2D still delivers (electromagnetic force, drag, lateral force distribution coefficient of pressure and speed on profile) with a confidence level high versus ease of use.

Acknowledgment

This article has received support from UEFISCDI through national project MASIM *"Multi Agent Aerial System with Mobile Ground Control Station for Information Management"*, PN-II-PT-PCCA-2013-4-1349.

References

1. https://www.aerodesign.de/english/profile/profile_s.htm. Accessed at 12.11.2016
2. Hepperle, M. (2014): *JavaFoil User's Guide*. Available at http://www.mh-aerotools.de/airfoils/java/JavaFoil%20Users%20Guide.pdf
3. Tsagarakis M. (2011): *Project Solaris – Analysis of airfoil for solar powered flying wing UAV*. Bachelor thesis, School of Innovation, Design and Engineering, Sweden
4. Duranti, S. (1995): *Profilli 2.21 help software*. Available at http://www.profili2.com/eng/default.htm
5. *** (2011): *Guidelines for XFLR5 v6.02, 2013*. Free software. Available at https://sourceforge.net/projects/xflr5/files/Guidelines.pdf/download
6. Prisacariu, V. (2013): *The aerodynamic analysis of the profiles for flying wings*. Journal of Defense Resources Management, ISSN 2068-9403, Vol. 4, no. 1(6), p211-218
7. http://airfoiltools.com/airfoil/details?airfoil=pw51-pw. Accessed at 14.11.2016
8. Wick, P. (2006): *Peter Wick on Planks. Part 3: The good slope plank*. In Radio Controlled Soaring Digest, Vol. 23, No. 3, p. 7-11, Available at http://www.rcsoaring.com/rcsd/RCSD-2006-03.pdf
9. Vural, M.: *Estimating R/C model aerodynamics and performance*. Available at https://mypages.iit.edu/~vural/RC%20Airplane%20Design.pdf
10. Prisacariu, V., Boşcoianu, M., Cîrciu, I. (2013): *Morphing wing concept for small UAV*. Applied Mechanics and Materials, ISSN 1662-7482, Vol. 332, p. 44-49, doi:10.4028/www.scientific.net/AMM.332.44 OPTIROB 2013, Trans Tech Publications, Switzerland
11. *XFLR5 Analysis of foils and wings operating at low Reynolds numbers,* Guidelines for QFLR5 v0.03, 2009, 58p, Available at https://engineering.purdue.edu/~aerodyn/AAE333/FALL10/HOMEWORKS/HW13/XFLR5_v6.01_Beta_Win32(2)/Release/Guidelines.pdf

Received in December 2017